

IN-FLIGHT EXPERIENCE OF THE HIGH PERFORMANCE ATTITUDE DETERMINATION AND CONTROL SYSTEM OF THE GENERIC NANOSATELLITE BUS

Karan Sarda⁽¹⁾, Alex Beattie⁽¹⁾, Daniel D. Kekez⁽¹⁾, Robert E. Zee⁽¹⁾

(1) Space Flight Laboratory, University of Toronto Institute for Aerospace Studies, 4925 Dufferin Street, Toronto, Ontario, Canada, M3H5T6, ksarda@utias-sfl.net, 416-667-7923

ABSTRACT

On July 12 2010 the first Generic Nanosatellite Bus (GNB) spacecraft, AISSat-1, was launched aboard a Polar Satellite Launch Vehicle rocket. The Generic Nanosatellite Bus is a 6.5-kg satellite platform which was designed, built and commissioned by the Space Flight Laboratory of the University of Toronto. AISSat-1's primary mission was to investigate the orbital reception of maritime Automatic Identification System (AIS) message traffic and demonstration of a high duty cycle operational space-based AIS service capability.

The GNB is a flexible, high-performance nanosatellite platform designed to support multiple missions with differing mission and payload requirements with minimal modification. In this way, mission cost, time from inception to flight, and risk is minimized by leveraging heritage from one mission to the next. This modular design philosophy is especially embodied in the attitude subassembly, which can meet the needs of a very wide variety of missions, ranging from those only requiring coarse determination and control through magnetic-field-tracking to high-performance three-axis systems requiring arc-minute level accuracy.

This paper will first summarize the GNB platform and the AISSat-1 mission, but will focus primarily on the GNB attitude subsystem. A review of the attitude sensors and actuators will be given, as well as an overview of the attitude software. With the foundation and context presented, a detailed treatment of the commissioning results and the attitude performance within the operational phase of the mission will round out the paper.

1 INTRODUCTION

In recent years, nanosatellite technology has matured to the point where it can now be used to enable aggressive, timely, and relevant missions for users whose only options previously were larger, more expensive satellites, or a non-satellite solution with much greater cost or lower coverage and flexibility. The Space Flight Laboratory (SFL) at the University of Toronto Institute for Aerospace Studies (UTIAS) has been a pioneer in nanosatellite technologies since the first 1-kg CubeSat satellites were conceived, designed and launched as part of the first CubeSat cluster launch in 2003. Since then, three more nanosatellites have been launched by SFL as summarized in Table 1.

Each mission has not only raised the bar in terms of technological maturity and performance, but also in the aggressiveness and import of the mission. Early nanosatellites, both from SFL and other organizations around the world, were primarily technology demonstrations. With AISSat-1, and the first deployment of the Generic Nanosatellite Bus (GNB) platform, pseudo-operational real-world

problems have now been demonstrably tackled by a nanosatellite platform.

Satellite	Launch Date	Mission
CanX-1	June 30, 2003	Technology Demo
CanX-2	April 28, 2008	Technology Demo, Atmospheric Science
NTS	April 28, 2008	Space AIS Investigation
AISSat-1	July 12, 2010	Space AIS Investigation, Operational Demo

Table 1: SFL Nanosatellite Launch History

Complete three-axis attitude control had traditionally been a challenge to implement at the nanosatellite level. Due to recent advances in miniaturization of critical pieces of hardware, notably reaction wheels, accurate three-axis control at this small scale is now finally a reality. The attitude subassembly of the generic nanosatellite bus, in particular, is considered amongst the current state of the art in terms of capability and accuracy.

This paper summarizes the GNB platform, with a strong focus on the attitude subassembly, along with an overview of the AISSat-1 mission. In-orbit commissioning and operations results of the attitude subsystem are presented.

2 THE GENERIC NANOSATELLITE BUS

The Generic Nanosatellite Bus is an advanced nanosatellite platform that was developed by SFL as an evolution of the older CubeSat-based missions. In addition to the satellite bus itself, the GNB platform also includes a baseline supporting ground segment implementation in order to provide a reliable, complete end-to-end system.

Knowledge and flight experience gained from the earlier programs, along with important input from users regarding what scope of platform would be useful for more demanding missions, was used to define the next-generation nanosatellite platform. The GNB was originally co-designed by two SFL programs with very different mission requirements:

- The Bright Target Explorer (BRITE). BRITE is a six-satellite optical space astronomy constellation formed by an international collaboration of Canadian, Austrian, and Polish teams each building two complete satellites.
- The CanX-4 and CanX-5 dual-satellite mission, which is an enabling technology demonstration performing autonomous precision formation flying.

As a result, the GNB platform can easily accommodate a wide variety of payloads and operational profiles with minimal modification to the core satellite bus. AISSat-1 is a very good example of this capability, as the mission was defined and implemented long after the GNB platform design was complete.

The GNB platform is a complete satellite system that can be tailored as needed to mission needs. The tailoring process is a combination of tailor-by-omission and tailor-by-modification approaches, with an emphasis on keeping design modifications to a minimum. This reduces overall schedule and cost, and minimizes the risks associated with design modifications to flight-qualified systems while maintaining the flexibility to address differing mission requirements.

The GNB is an advanced ~6 kg nanosatellite platform in a 20-cm cubic form factor. It is designed such that the bulk of the bus electronics are generic, and their accommodation in the satellite does not change from mission to mission. An example of two fully assembled GNB satellites, AISSat-1 and the first BRITE, is shown in Figure 1.

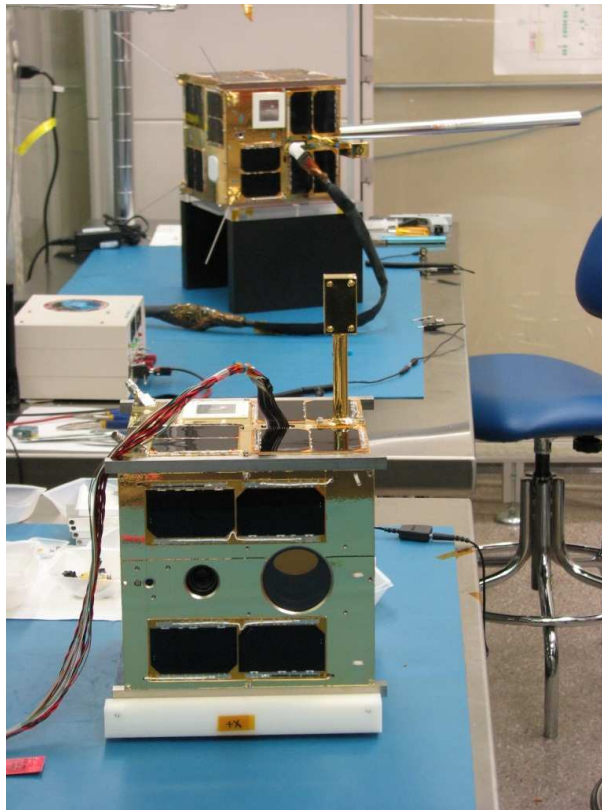


Figure 1: AISSat-1 (background) and BRITE (foreground)

The internal structural concept is shown in Figure 2. The platform is designed around two structural trays that house the majority of the satellite electronics, including all of the generic bus systems, around which are attached panels housing additional functionality. In addition to bus systems, additional space in these trays is available for payload support electronics (e.g. a dedicated payload computer) as needed on a mission-by-mission basis. Only minimal modification of the structure is typically necessary for different missions.

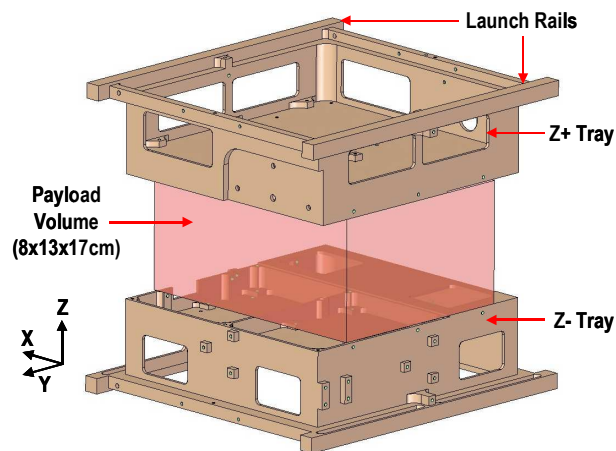


Figure 2: GNB Structural Concept

The main payload area is located in the centre volume of the satellite. A large proportion of the

satellite's volume is available for use by the payload, and it is constrained only in a simple shape and mounting method. This allows great flexibility in accommodating different payloads. Locating the payload in the centre of the satellite also provides a very stable thermal environment, and access to four different surfaces for payload elements that must protrude through or have visibility beyond the outer structure of the satellite, such as antennas and instrument apertures.

The platform contains all the elements necessary for a wide variety of missions, including:

- Dual, redundant 5.2 A-hr batteries with independent charge/discharge regulation
- Body-mounted solar arrays providing power generation in all attitudes
- Dual parallel and interchangeable 60 MHz on-board computers, normally dedicated to housekeeping and attitude control duties, respectively
- Customizable payload control and data processing computer, up to 1 GB of storage
- Omni directional 4 Kbps UHF command uplink
- Omni directional S-band telemetry and payload data downlink (up to 1 Mbps, commandable)
- Hemispherical coverage GPS receiver for positioning and timing
- Full attitude determination and control system, based on a customizable suite of sensors (sun sensors, rate sensors, magnetometer, star tracker) and actuators (reaction wheels, magnetorquers). Multiple control modes are available (e.g. inertial, orbit-frame-tracking).

Functionality that is not needed for a given mission can be omitted. For example, if a mission does not require high precision attitude control the star tracker may be omitted.

The GNB platform is designed to allow a high degree of operations flexibility and autonomy. A typical GNB mission will require much less than one full time operator to task, monitor, and maintain the system. Payload operations are typically scheduled either by an on-board scheduling mechanism or via time tagged scripts that are pre-generated by a ground tasking system and uploaded to the satellite in advance. The on-board time-tagging system allows a high degree of control and can support easy insertion of new commands at any time to allow emergency or limited-opportunity activities on short notice.

Further details regarding other GNB-based missions can be found in [1] through [3].

3 THE ATTITUDE SUBASSEMBLY

The key to a multi-mission design, such as is the case for the broad intentions of the GNB class of satellites, is the ability to easily tailor a common idea to a particular case, which reduces the associated non-recurring engineering costs, project schedule and mission risk. In any given mission that requires an attitude assembly, there are three basic elements: the sensors that measure certain phenomena; software that processes these measurements and calculates corrective action; and actuators that implement the calculated thrust and or torque commands. Tailoring of the hardware involves selection of appropriate sensors and actuators that enable the fidelity of the given case's knowledge and control requirements. The software, on the other hand, should be designed to essentially be independent of which sensors have been chosen, save, perhaps, for minor implementation specifics. This is the basic design approach adopted in developing the attitude subassembly for the GNB class.

The multi-mission-design architecture for the GNB attitude subassembly is shown in Figure 3, where the On-Orbit Attitude Subsystem Software (OASYS), which is comprised of an extended Kalman filter (EKF), and a set of control laws is constant for every mission. All control laws fly for all missions, however, which ones are actually available and used depends on the particular mission needs and hardware complement. Which sensors and actuators are incorporated depends on the mission. Specific

components can be added or subtracted with minimal interfacing effort, giving both the software and hardware significant modularity.

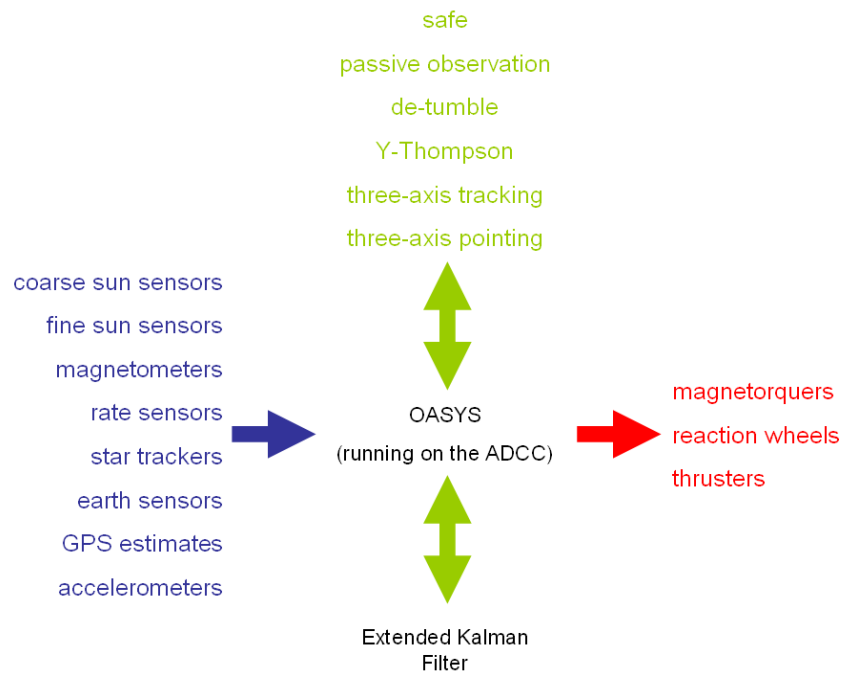


Figure 3: Basic Flow Diagram for the Multi-Mission GNB ADCS Architecture

OASYS (On-board Attitude SYstem Software) is the flight software that performs all the necessary computations for attitude determination and implements attitude-control laws to achieve a desired attitude state (attitude quaternion, and angular velocity in the body frame of reference). It is in part comprised of a satellite-position propagator, a solar ephemeris and an IGRF-11, magnetic-field, model of the Earth. These models are used in conjunction with sensors to estimate the satellite’s attitude by means of an Extended Kalman Filter (EKF). The control laws are then implemented based on the estimated state. The attitude software is run at a fixed-but-configurable frequency of 0.5Hz on a dedicated Attitude Determination and Control Computer (ADCC). Each 2 s frame has a series of events, the order of which does not change: read sensors, run OASYS and command the actuators.

As illustrated in Figure 3, the ADCS of the GNB can support a wide range of attitude hardware. Much of this hardware is developed in-house by SFL. Examples of SFL-built hardware include digital sun sensors, three-axis magnetometers, three-axis rate sensors, cold-gas thrusters, vacuum-core magnetorquer coils, and on-orbit attitude computers. SFL, in partnership with Sinclair Interplanetary have also developed a range of reaction wheels. In another partnership, SFL, Sinclair Interplanetary, and Ryerson University’s SAIL laboratory developed a low-cost high performance star tracker, which the first will fly on a SFL GNB satellite in Q4 2012.

The SFL-built sun sensors are a combined coarse (phototransistor based) and fine (digital-pixel array based) sun-sensor circuit is used to measure the local sun vector. The primary function of the coarse sun sensors is to select a fine sun sensor to use for attitude determination, which is desirable because readout times for the fine sun sensors are appreciable, relative to an attitude cycle. The fine sun sensor is based on a CMOS area sensor that outputs two one-dimensional profiles. The output profiles show intensity along the sensor’s 1 and 2 directions. Centroid algorithms in OASYS then determine the estimated location of the sun spot on the 2D array.

The GNB magnetometer is a three-axis, boom-mounted, sensor that provides measurement of the local

magnetic field for comparison with an on-board IGRF-11 magnetic-field model. The magnetometer relies on three orthogonal magneto-inductive sensors. These sensors are designed to alter their inductance in the presence of magnetic fields. SFL's GNB rate sensors employ micro-electro-mechanical-system (MEMS) rate sensor heads, which rely on the Coriolis Effect. In these sensors, a proof-mass is oscillated along one axis creating a periodic velocity. Any rotation about a perpendicular axis will create Coriolis acceleration in an axis that is perpendicular to both the rotation and the driving vibration. The displacement due to the Coriolis acceleration is determined through capacitance measurement.

Reaction wheels are the primary means of actuation for the GNB. A wide range of wheels were developed in partnership between SFL and Sinclair Interplanetary, with momentum capacities from 7mNms to 1Nms. The GNB nominally employs three 30mNms wheels arranged orthogonal to each other, producing a nominal torque of 2mNm per axis. In order to trim momentum levels in the wheels, and to damp spacecraft body-rates, the GNB employs three orthogonal vacuum-core, electromagnetic coils, commonly referred to as magnetorquers. The power supplied to the GNB magnetorquers is current-controlled, removing underlying compensation calculations that are otherwise necessary for resistance (which changes with temperature).

A host of control laws have been designed within OASYS to enable a very wide range of missions, however a fundamental suite of three are predominantly used. This includes the B-dot magnetic controller that requires only knowledge of the rate of change of the local magnetic field in the body frame, to null body-rates. Second, in order to prevent the saturation of the reaction wheels, through the action of secular disturbance torques, a magnetic momentum management controller, of the form of a simple proportional controller acting on the error relative to a reference momentum is used. Third, in order to actually point the GNB, a three-axis controller in the form of a linear quaternion and linear body-rate feedback PID controller is used. This near-minimum-time eigen-axis rotation controller is capable of holding to an inertially-fixed target, or given a set of roll, pitch and yaw angles, tracking a fixed target relative to the moving classical orbit frame.

4 AISSAT-1

AISSat-1 is a Norwegian nanosatellite, funded by the Norwegian Space Centre and managed by the Norwegian Defence Research Establishment (Forsvarets Forskningsinstitutt, FFI). FFI also maintains the Mission Control Centre (MCC) for the satellite and performs all mission operations. The satellite bus was designed and manufactured by SFL, and all satellite assembly, launch, and commissioning activities were conducted by SFL with support from FFI for payload activities. The payload electronics module was designed and built by Kongsberg Seatex in Norway.

AISSat-1's mission is to investigate the ability of a satellite platform to receive data from the maritime Automatic Identification System (AIS) and to demonstrate how this data can be disseminated and used by end-users in an operational system. The primary area of interest is the Norwegian coastal waters and areas of the High North under Norwegian authority. These are large areas of open-ocean, much of which was previously not actively monitored on a regular basis.

AISSat-1 was designed with a full complement of GNB hardware and software in addition to its payload elements, with the exception of a star tracker which was not required. Therefore, the attitude system hardware was comprised of six digital sun sensors, one boom-mounted three-axis magnetometer, and one three-axis rate sensor to round out the determination suite. For control AISSat-1 employs three miniature reaction wheels and three vacuum-core magnetorquer coils.

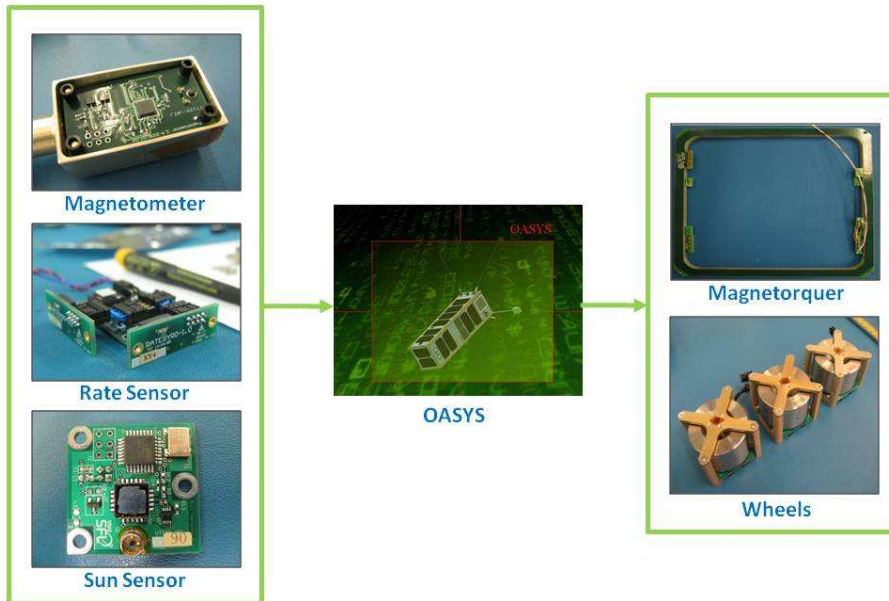


Figure 4: AISSat-1 ADCS Configuration

Demonstrating the advantages of the GNB design approaches, AISSat-1 was completed in a truncated satellite development program with the preliminary design phase omitted and the critical design phase highly accelerated.

Further details on AISSat-1's mission and payload can be found in [4] and [5].

5 LAUNCH AND EARLY OPERATIONS

AISSat-1 was launched on the Indian Polar Satellite Launch Vehicle, as part of SFL's Nanosatellite Launch Service 6 (NLS-6) cluster, on July 12, 2010. AISSat-1 and its separation system were accommodated on the PSLV's upper stage equipment deck as shown in Figure 5.

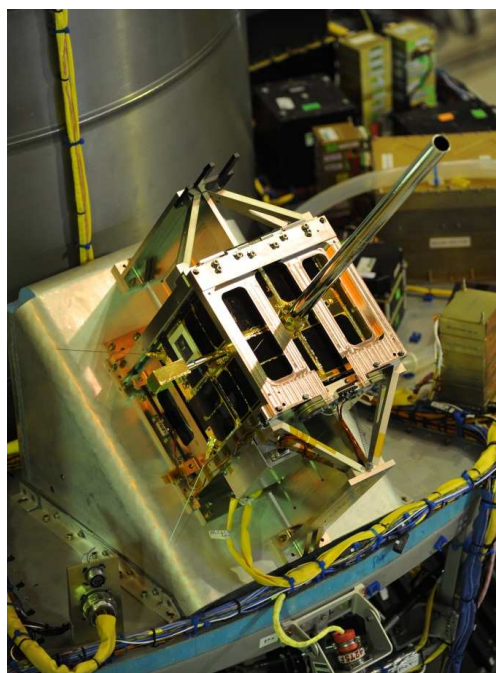


Figure 5: AISSat-1 in launch configuration.

The target orbit, a 635 km sun-synchronous orbit with a descending node of 10:00, was achieved precisely. The satellite was deployed over the southern Indian Ocean, not far from the coast of Antarctica.

Due to the locations of AISSat-1's Earth stations, initial acquisition occurred only a short time later. Initial telemetry indicated a fully successful and healthy delivery into orbit. The satellite was commandable and responsive. The power system was operating as expected, with expected levels of power generation observed. The thermal state of the spacecraft was in line with thermal model expectations. The main housekeeping computer was healthy, storing telemetry and handling command requests properly, and ready to support higher levels of operations

Owing to the excellent early operations results, the AISSat-1 payload was activated in its real-time mode for the first time less than 12 hours after initial acquisition and the system was able to receive and disseminate live AIS message traffic from the High North immediately. Thus in a very short time the mission was able to complete a number of critical mission milestones and demonstrate high confidence in the larger mission.

6 ATTITUDE SUBSYSTEM COMMISSIONING

The attitude determination and control subsystem (ADCS) was commissioned in three main phases. The first was a verification of the determination and control hardware, followed by a checkout of the attitude solution, and finally an evaluation of each control algorithm. These activities were performed largely in parallel with other commissioning activities.

6.1 ADCS Hardware Checkout

The checkout of the determination hardware was successful with the hardware operating within expectations. The sun sensor dark noise metrics were within expected limits and solar response and field of view was affirmed. Magnetometer noise was low and in line with expectations, at 0.2° per axis (1-sigma). The measured magnetic field magnitude was in line with accurate ephemerides, thus indicating that the measurement of the boom-mounted magnetometer was not impinged by spacecraft residual or dynamic dipoles. The rate sensor noise was acceptably low and matched pre-launch statistics, at less than $0.06^\circ/\text{s}$ (1-sigma). The measurement of the rate sensor was well correlated against those inferred from finding the period of harmonic oscillation of the magnetometer.

Prior to running attitude estimation algorithms on-board, much of the attitude state was inferred by the rate sensors and magnetometers. In particular, it was possible to determine the initial kick-off tumble rate was $\sim 6^\circ/\text{s}$.

The control hardware checkout was conducted in parallel with the attitude determination algorithm evaluation. The performance of the vacuum core magnetorquer coils was investigated by comparing the actual measured body-rate profile versus that expected given the magnetic field measurements, and measured torque current. This comparison yielded a strong correlation, thus indicating that the torquers were performing well, and were imparting a torque on the order of 10^{-5} Nm at the AISSat-1 orbit altitude.

The reaction wheel checkout involved spinning the wheels up to 300rad/s and allowing them to coast back to zero. From this data, the wheel viscous damping coefficient, attitude rate estimation performance, and the moment of inertia of AISSat-1 were investigated. Measuring the viscous damping coefficient is one of the most meaningful indicators on how well the wheel bearing

survived launch, where a large change would indicate some mechanical impact. On-orbit spin-down testing confirmed that the coefficients for each wheel were nearly identical to the pre-launch measurements. The spin-down tests also provide an estimate of the satellite inertias, which matched the results of coarse pre-launch testing.

6.2 Attitude Solution Verification

The attitude determination algorithm of the on board attitude software, OASYS, is comprised of three main parts: first, a set of ephemerides to calculate the expected measurement vectors, second, sensor processing to take the raw measured readings and construct an actual measured vector, and third an EKF that compares the two sets of vectors and yields a state estimate. In addition, the software is equipped with a host of error reporting arrays that indicate issues encountered in any particular control frame.

The on-board SGP4 position, IGRF magnetic and C-24 solar ephemerides were found to be well correlated when compared against more accurate sources at the recorded time stamps. A review of sensor processing confirmed the accuracy of several key sensor calibration values. For example, the magnetometer bias and scale factor were verified by plotting each axis of the magnetometer relative to another during the wheel spin tests. These plots, from a well calibrated magnetometer, should result in an ellipse with an origin and eccentricity near zero. A plot of the magnetometer Z versus X-axis during a wheel spin up is shown in Figure 6.

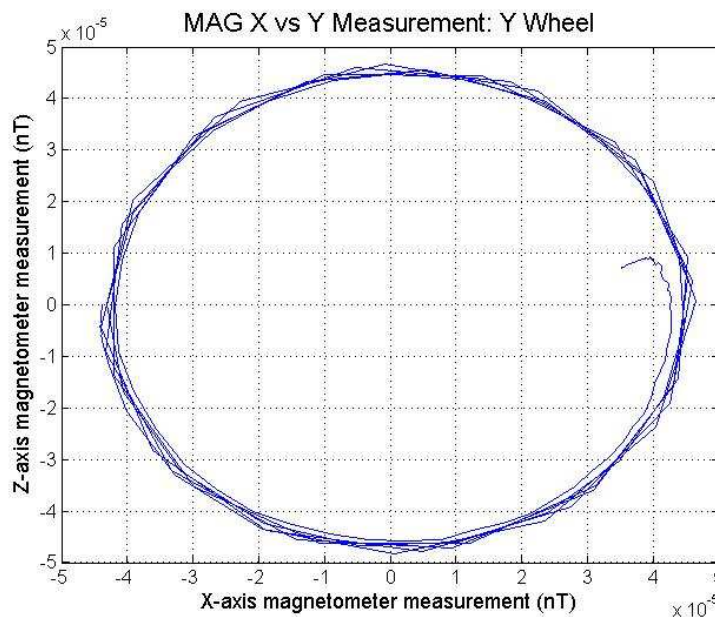


Figure 6: Magnetometer Z-axis versus X-axis during the Y-wheel spin up test

The attitude solution estimated by the EKF was investigated by comparing the quaternion estimate against that from the TRIAD algorithm [6]. TRIAD is a deterministic quaternion solution that utilizes the sensor measured body-frame vectors and the ephemerides calculated inertial-frame vectors. It is important to note that this analysis simply affirms that, given the sensor measurements, the estimate generated by the EKF of OASYS is reasonable. Unfortunately, a true checkout of the state estimate performance on AISSat-1 cannot be conducted due to a lack of an absolute truth model. Such evaluations of filter performance are characterized in simulation only where the filter estimate, which is based upon corrupted sensor measurements, is checked against a simulated truth.

Figure 7 shows the angular difference between the OASYS and TRIAD estimates. The correlation is quite good, indicating that the filtered estimate is valid. The angular difference between the two is typically less than 5° with a root mean square (RMS) of less than 2° , except for occasional instances of poor sun sensor readings where the solar cell current is used to generate a coarse sun vector estimate instead. In some instances the use of direct measurements in the TRIAD solution causes sharp shifts in the angular difference, particularly as the sun enters the field of view of one sun sensor and leaves the other. Each sun sensor has unique calibration values and unique error properties as a result. The EKF, being a low-pass filter, will correctly filter this whereas the TRIAD solution will suffer. Largely, the angular difference between the TRIAD and OASYS quaternion solution is due to the EKF minimizing the estimated error covariance, whereas the TRIAD solution uses the corrupted sensor measurements directly.

The filter can also be assessed by surveying the Kalman filtering performance indicators. The first is an investigation of the statistics of the sensor residuals. A residual is defined as the difference between the projected state estimate (actual measurement) and the expected measurement (ephemeris calculated result, rotated by the inertial-to-body rotation matrix). The extended Kalman filter is built on the principle that these errors are zero-mean and Gaussian. The means of the magnetometer, rate sensor and sun sensor residuals were computed, and were found to be essentially zero. Further, it can be shown that the sensor residual must always be within the 68% of the expected value. The residual expected value is proportional to the root of the sensor error noise covariance, the process noise covariance, and the estimated state covariance [7]. A plot of actual and expected value of the magnetometer and rate sensor residuals is shown in Figure 8 and Figure 9. In all plots, the residual is below the expected, which is the desired result, indicating that the filter is working and tuned fairly well.

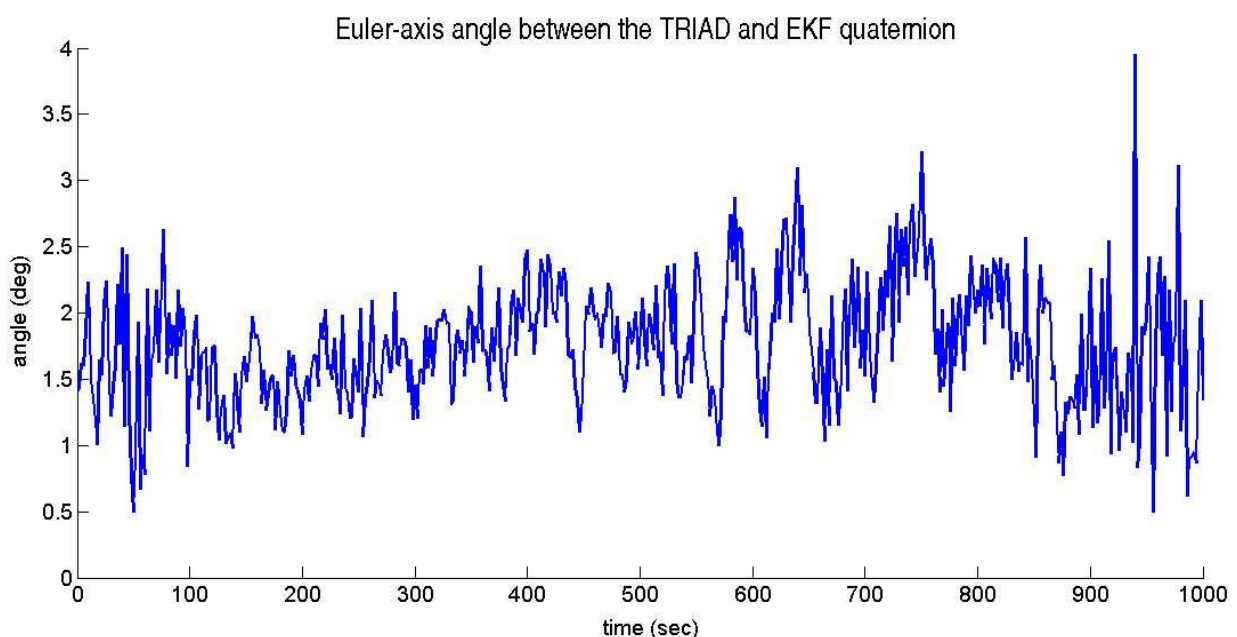


Figure 7: Angular difference (euler-axis angle) between the TRIAD generated and OASYS estimated quaternion

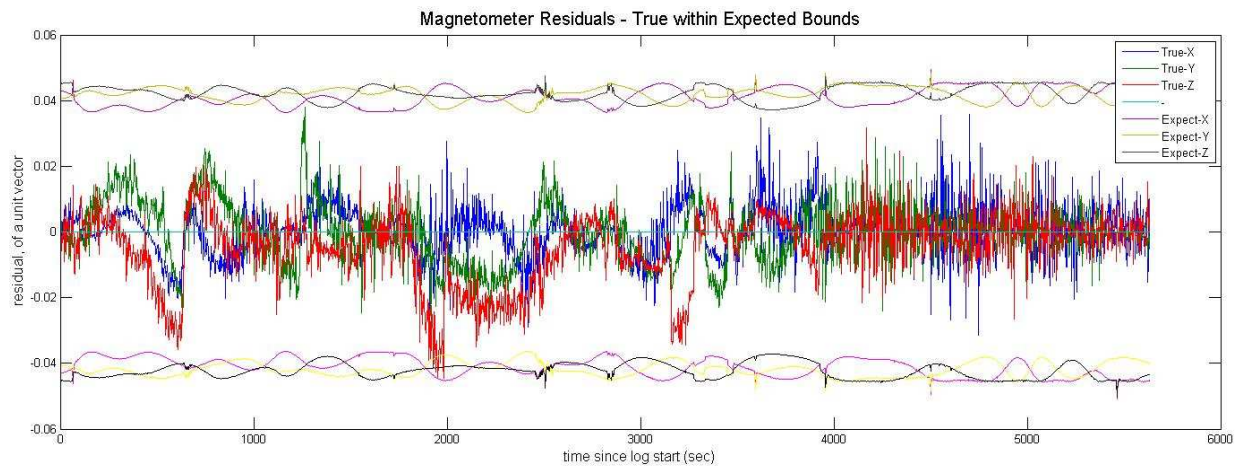


Figure 8: Actual and expected value of the residuals during the magnetometer update step of the EKF

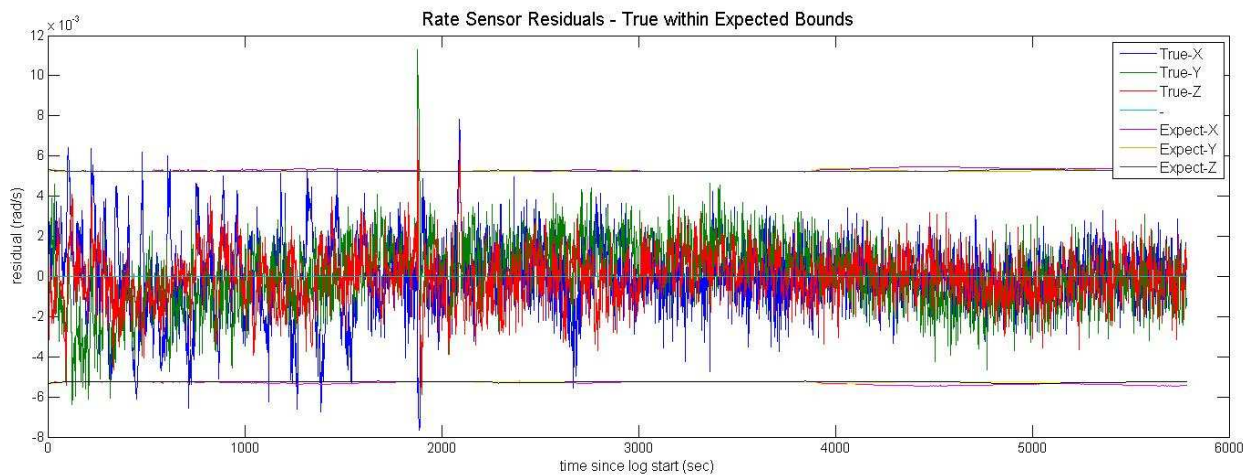


Figure 9: Actual and expected value of the residuals during the rate sensor update step of the EKF

6.3 ADCS Control Algorithm Performance

The attitude software, OASYS, is equipped with a host of control algorithms applicable to a variety of mission; however, the AISSat-1 mission only requires the regular use of a subset. The B-dot rate damping controller is used to minimize body-rates. A three-axis quaternion feedback controller is used to either align the spacecraft frame in an orientation fixed in the inertial frame (inertial-pointing), or an orientation fixed in the moving orbit frame (orbit-tracking). Wheel momentum management is continuous and is a sub-mode of the spacecraft three-axis controller.

The B-dot body-rate damping controller, which operates on the rate of change of the measured magnetic field measurements alone, was demonstrated successfully to reduce rates to nearly the theoretical limit of approximately two rotations per orbit, or $0.13^\circ/\text{s}$. Figure 10 illustrates an example when the B-dot controller was used to damp rates from approximately $4.3^\circ/\text{s}$ to nearly this limit in 1500 OASYS cycles, or 3000 seconds. AISSat-1 has since used its B-dot controller to damp rates of $25^\circ/\text{s}$ in less than an orbit.

Three-axis inertial-pointing performance of AISSat-1 was investigated by commanding four sequential quaternion targets, each separated by a span of 600 seconds. These targets were designed to initially place AISSat-1 in an attitude with only two body-faces illuminated, with one at a 30° angle of incidence to the sun and the other at 60° . From that initial attitude, the spacecraft was commanded to first rotate 90° about the +Z-axis, then $+90^\circ$ about the +Y-axis and then $+90^\circ$ about

the +X-axis. Figure 11 shows the satellite tracking the sequence of commanded targets, including the slews. The time taken to reach the 2% settling band for these three 90° slews were 85 seconds on average. An example of the body-rate profile during one of the slews is shown in Figure 12.

Due to a lack of a truth model, absolute accuracy of the AISSat-1 attitude controller cannot be precisely determined. Accuracy, though, can coarsely be affirmed by analysing the sensor measurements at each target. First, using the sun sensor and magnetometer measurements as well as the corresponding ephemerides-generated vectors, the TRIAD algorithm can again be employed to generate the inertial-to-body-frame quaternion. This, sensor-measurement based quaternion can then be compared against the commanded state. The Euler-axis angle between these two frames was computed for each of the four targets, where the results for target two are plotted in Figure 13, and the results for all four targets are summarized in Table 2.

The root mean square errors are less than 2.4°. Further, a comparison between the expected solar and magnetic field measurements and the actual sensor measurements was conducted for each of the four targets. The results of this analysis are tabulated in Table 3 and Table 4. The results indicate that the apparent root mean square sun sensor and magnetometer error is less than 2.1° and 1.6° respectively. This error includes all error sources of each sensor, that is, noise, misalignment, and accuracy; however, this error measurement will be corrupted by sensor bias.

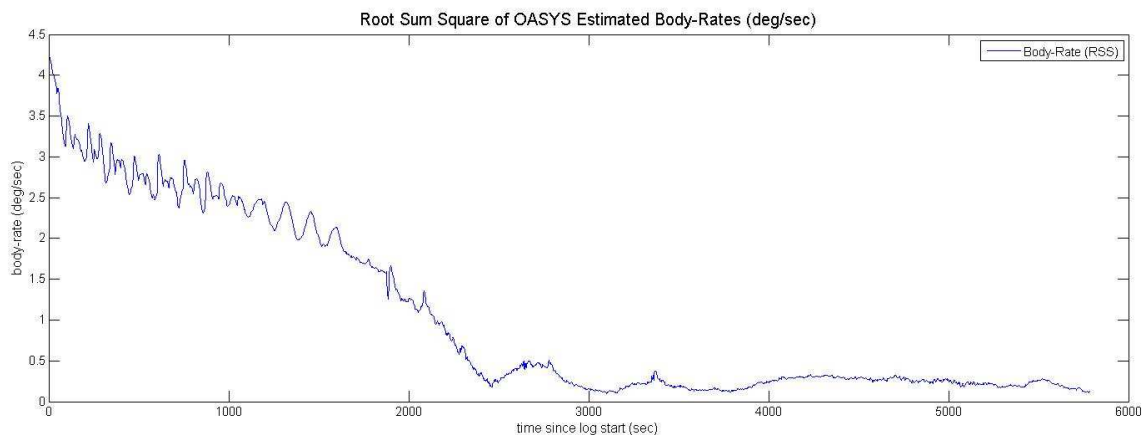


Figure 10: Body-rate profile during the action of the B-dot rate damping controller

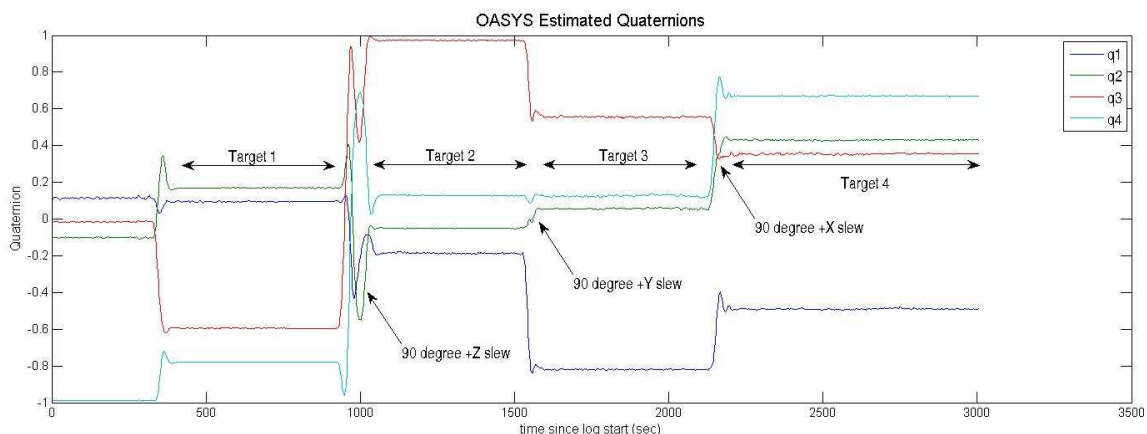


Figure 11: OASYS estimated quaternions during the three-axis inertial pointing checkout

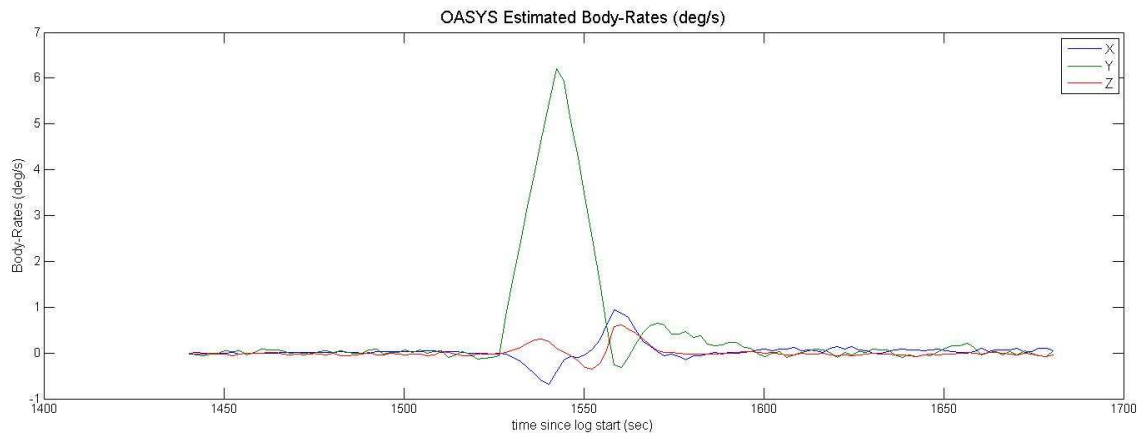


Figure 12: Estimated body-rate profile during the Y-axis slew

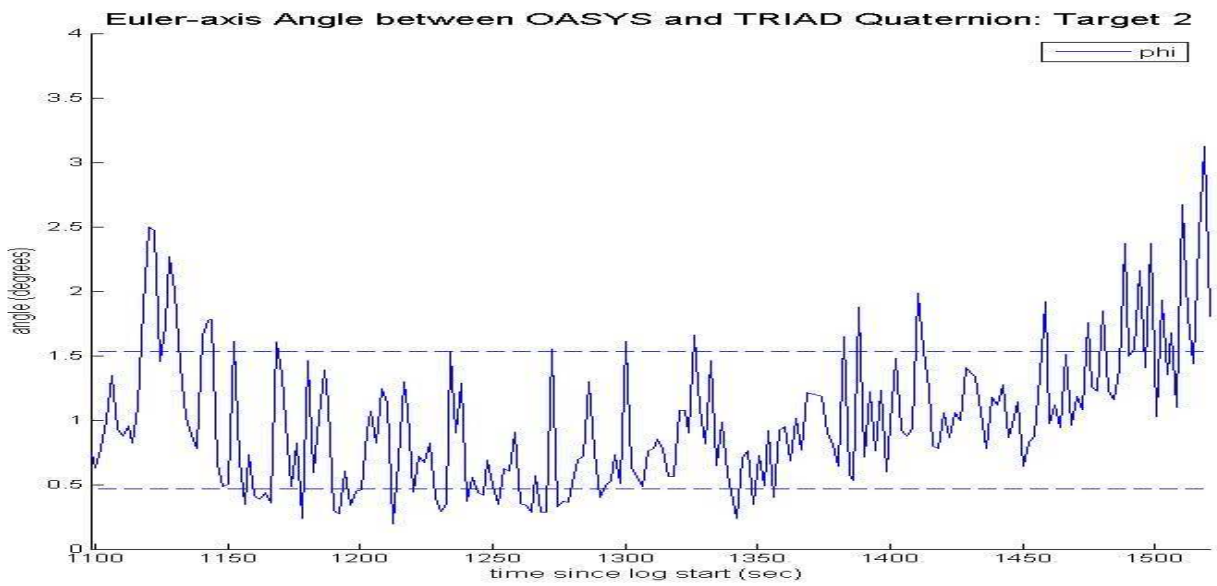


Figure 13: Euler-axis angle between the OASYS and TRIAD quaternion

Target	μ (degrees)	σ (degrees)	RMS (degrees)
1	1.29	0.56	1.41
2	1.00	0.53	1.13
3	2.35	0.48	2.39
4	1.72	0.88	1.92

Table 2: Root mean square of Euler-axis angle between OASYS and TRIAD generated quaternion for inertial-pointing targets 1 through 4

Target	μ (degrees)	σ (degrees)	RMS (degrees)
1	1.12	0.63	1.29
2	0.57	0.33	0.66
3	2.03	0.42	2.08
4	0.86	0.32	0.92

Table 3: Root mean square of angle between expected and measured solar vectors for inertial pointing targets 1 through 4

Target	μ (degrees)	σ (degrees)	RMS (degrees)
1	1.34	0.58	1.46
2	0.73	0.41	0.84
3	1.41	0.74	1.59
4	1.11	0.54	1.23

Table 4: Root mean square angle between expected and measured magnetic field vectors for inertial-pointing targets 1 through 4

AISSat-1 normally employs the orbit-tracking mode of the ADCS, which was verified after the inertial pointing mode. The operational desire is to orient the payload antenna in a fixed orientation relative to the orbit frame. The orbit-tracking algorithm was verified by comparing the measured solar and magnetic field vectors against the expected. Results indicated that the root mean square difference of the expected and measured sun sensor and magnetometer measurements were 1.8° and 1.5° respectively. Further, the angle between the expected quaternion and the TRIAD-generated quaternion was 2.2° . Note, the angular difference between the EKF-estimated quaternion and the expected quaternion was obviously much smaller (small fractions of a degree), as this is the metric which is being minimized by the three-axis quaternion feedback controller, and thus cannot be used for a performance metric.

Finally, the momentum management controller for AISSat-1 is designed to maintain the wheel rate to a reference rate of ± 50 rad/s in the body-frame. As the plot in Figure 14 indicates, the wheel speed is bounded over time and therefore the momentum management controller is working well in maintaining a reference angular momentum.

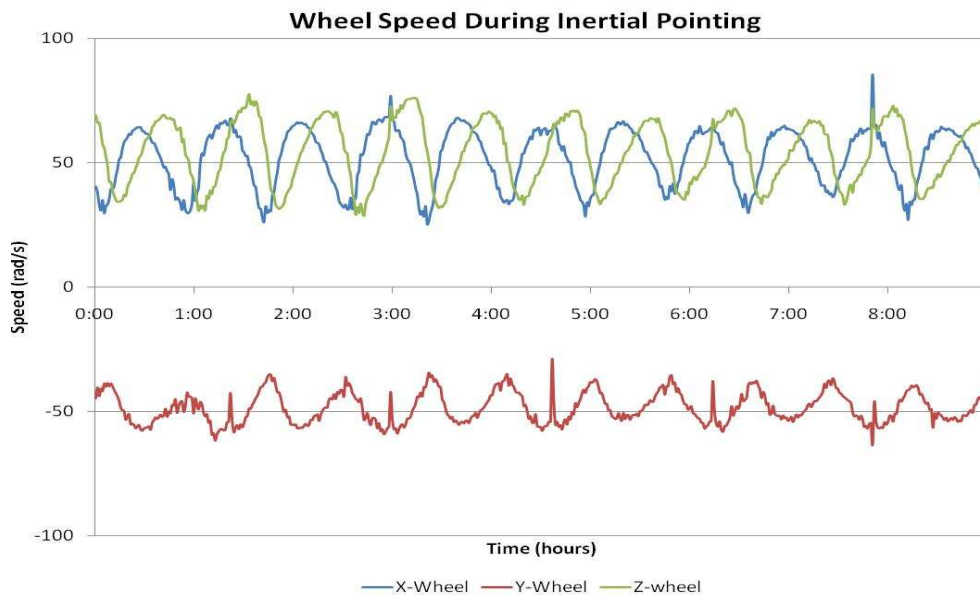


Figure 14: Wheel speed while holding an inertial target over a span of 9 hours

7 CONCLUSION

AISSat-1 and GNB platform commissioning was formally concluded on November 26, 2010 in a handover ceremony where Norwegian authorities took over full operational responsibility for the mission.

With the successful implementation of the AISSat-1 mission, the GNB platform has been verified and the broader utility of capable nanosatellite platforms in solving operationally-relevant real-

world problems has been demonstrated. The AISSat-1 mission has demonstrated that a high degree of operational reliability can be obtained in a low-cost, high-performance nanosatellite platform. As of the time of writing, the satellite continues to provide mission data to its end users and operates in a pseudo-operational fashion. A second satellite, AISSat-2, is now under construction to provide additional system uptime at a fraction of the cost of a larger satellite or ground-based system.

The attitude subsystem of the SFL's Generic Nanosatellite Bus can support a wide range of missions, as well as a range of platforms, as the GNB subsystem was recently extrapolated for use for SFL's third generation nanosatellite bus, the NEMO-class bus, which is a 15-kg nanosatellite, and ComDev's AIM-class 70-kg microsatellite bus. The GNB ADCS is now flight proven with currently nearly 2-years experience on the AISSat-1 mission, and significant aspects of the attitude system have over four years of flight heritage on SFL's CanX-2 technology demonstration mission [8]. A series of GNB satellites are now fully funded and expected to launch within the next 2 years as summarized in Table 5. AISSat-1 has provided significant assurance in the platform that forms the basis for all of these missions. The presence of a star tracker on the BRITE series of satellites will allow even further evaluation and verification of the performance of the GNB ADCS, with pointing demonstrated at the arc-minute level, as discussed in [9]. Further, CanX-4/-5 formation flying satellites will demonstrate rapid & agile target tracking performance, by continuously slewing large angles in very short time-scales.

Satellite	Launch Date	Mission
UniBRITE	Q4 2012	Stellar photometry
BRITE-Austria	Q4 2012	Stellar photometry
BRITE-Poland 1	Q4 2012	Stellar photometry
CanX-4/-5	2013	Formation flying
AISSat-2	2013	Space AIS monitoring
BRITE-Canada-1/-2	2013	Stellar photometry
BRITE-Poland 2	TBC	Stellar photometry

Table 5: Forthcoming GNB Launches

8 REFERENCES

- [1] Deschamps, N., et al., *The BRITE Space Telescope: A Nanosatellite Constellation for High-Precision Photometry of the Brightest Stars*, 20th Annual AIAA/USU Conference on Small Satellites, Logan, Utah, August 2006.
- [2] Orr, N., et al., *Precision Formation Flight: The CanX-4 and CanX-5 Dual Nanosatellite Mission*, 21st Annual AIAA/USU Conference on Small Satellites, Logan, Utah, August 2007.
- [3] Bonin, G., et al., *The Antarctic Broadband Demonstration Nanosatellite: Fast Internet for the Bottom of the Earth*, 25th Annual AIAA/USU Conference on Small Satellites, Logan, Utah, 2011.
- [4] Narheim, B., et al., *A Norwegian Satellite for Space-Based Observation of AIS in the High North*, 22nd Annual AIAA/USU Conference on Small Satellites, Logan, Utah, August 2008.
- [5] Narheim, B., et al., *AISSat-1 Early Results*, 25th Annual AIAA/USU Conference on Small Satellite, Logan, Utah, August 2011
- [6] Wertz, J.R., *Spacecraft Attitude Determination and Control*, 1st Edition, December 31, 1980
- [7] Zarchan, P., Musoff, H., *Fundamentals of Kalman Filtering: A Practical Approach*,
- [8] Sarda, K., et al., *Canadian Advanced Nanospace Experiment 2 Orbit Operations: Two Years of Pushing the Nanosatellite Performance Envelope*, European Space Agency Small Satellite Systems and Services Symposium, Funchal, Madeira, Portugal, August 2010
- [9] Johnston-Lemke, et al., *Arc-Minute Stability on a Nanosatellite: Enabling Stellar Photometry on the Smallest Scale*, 25th Annual AIAA/USU Conference on Small Satellites, Logan, Utah, 2011